Optical properties of nanostructured TiO_2 thin films and their application as antireflection coatings on infrared detectors

R. C. Jayasinghe,[1] A. G. U. Perera,[1,*] H. Zhu,[2,3] and Y. Zhao[2]

[1]*Department of Physics and Astronomy, Georgia State University, Atlanta, Georgia 30303, USA*

[2]*Department of Physics and Astronomy, University of Georgia, Athens, Georgia 30602, USA*

[3]*School of Physical Science and Technology, Southwest Jiaotong University, Chengdu 610031, China*

**Corresponding author: uperera@gsu.edu*

Received July 30, 2012; revised September 7, 2012; accepted September 12, 2012;
posted September 13, 2012 (Doc. ID 173470); published October 11, 2012

Oblique-angle deposited titanium dioxide (TiO_2) nanorods have attracted much attention as good antireflection (AR) coating material due to their low n profile. Therefore, it is necessary to better understand the optical properties of these nanorods. TiO_2 nanorods grown on glass and Si substrates were characterized in the visible (0.4–0.8 μm) and infrared (2–12 μm) regions to extract their complex n profiles empirically. Application of these nanorods in multilayer AR coatings on infrared detectors is also discussed. Optimization of graded index profile of these AR coatings in the broad infrared region (2–12 μm) even at oblique angles of incidence is discussed. The effective coupling between the incoming light and multiple nanorod layers for reducing the reflection is obtained by optimizing the effect from Fabry–Perot oscillations. An optimized five-layer AR coating on GaN shows the reflectance less than 3.3% for normal incidence and 10.5% at 60° across the whole 2–8 μm spectral range. © 2012 Optical Society of America

OCIS codes: 310.0310, 310.1210, 310.6860, 310.4165.

In semiconductor detectors, there is significant amount of reflection (up to 30% depending on the refractive index (n) of the medium and the wavelength range) from the top surface. This will reduce the light throughput to the detector and also the field of view. Use of graded-index layers for broadband antireflection (AR) properties is one of the best approaches to reduce reflection. This was not feasible due to the unavailability of optical material with very low refractive indices. However, recent developments [1,2] in growth of titanium dioxide (TiO_2) and silicon dioxide (SiO_2) nanorods deposited by oblique angle deposition (OAD) have shown very low refractive indices close to air. This has the potential for broadband multilayer AR coatings. The proposed AR coatings will also be useful for enhancing the quantum efficiencies of solar cells and eliminating the need for tracking the moving sun. Another application is improving reflectance of Bragg reflectors by increasing the difference of refractive indices between two media.

Using OAD technique, an array of well-aligned and tilted TiO_2 nanorods has been fabricated by electron beam evaporation method on glass and silicon substrates [2]. The nanorod tilting angle with respect to the substrate normal increases with the increase of vapor flux angle ϕ_f [3]. The porosity of these layers increases with the ϕ_f and consequently decreases the effective n of the medium. The intensity-transfer matrix method [4] was used to calculate reflectance and transmittance spectra from the three phase vacuum/film/substrate structure. The multiple reflected beams from the substrate surfaces are added incoherently to neglect the phase information [5]. The transmittance spectra of TiO_2 films on glass are shown in Fig. 1(a). The nominal thickness of the thin films is 2 μm. The transmittance spectra show many peaks and valleys due to Fabry–Perot (FP) oscillations. It is seen that transmittance increases with the increase of ϕ_f.

In order to find the complex n of the nanorod thin film, the measured transmission data were fitted with calculated spectra. In the fitting procedure, first the real part of n is interpolated from the values reported in [1] for different ϕ_f. Then the thickness of the layer was varied around the nominal thickness (2 μm) until an approximate fit to the FP peaks is observed. Next, real part of n is varied slightly to better match the FP peaks with the experimental data. These fitting results are shown in Figs. 1(b) and 1(c) for different ϕ_f. The low amplitudes of the FP peaks in the experimental spectra could be due to the light scattering in the high energy region. The extracted real part of n values are plotted in Fig. 2(a) along with the best fit line. The effective n of TiO_2 films decreases with the increase of flux incident angle. The attenuation effect in transmission spectra is due to the

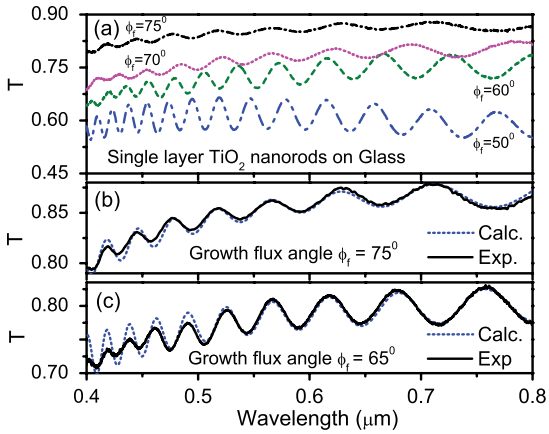

Fig. 1. (Color online) (a) Transmittance spectra of single layer TiO_2 nanorod films deposited at different vapor flux angles (ϕ_f). The transmission increases with increase of deposition angle. Comparison of experimental transmission data with calculations for ϕ_f of (a), (b) 75° and (c) 65° on glass substrate.

 © 2012 Optical Society of America

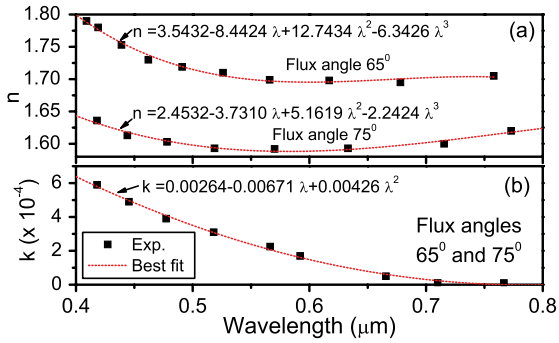

Fig. 2. (Color online) (a) Real (n) and (b) imaginary (k) parts of n determined by matching the FP peaks at different wavelengths. The dots represent the value at each FP peak. The best fit line was used to find the values at intermediate wavelengths. Imaginary part is the same for both the samples.

imaginary part of n. The value of this was found by matching the average height of the FP peaks with the experimental data. These values are plotted in Fig. 2(b). Both samples (ϕ_f 65° and 75°) have the same attenuation.

For TiO_2 nanorods grown on undoped Si substrate, n of the substrate is larger than that of nanorod thin film. Therefore, the reflection from the air/TiO_2 nanorod interface is less than that of air/Si interface. In other words, TiO_2 nanorod layer can act as an AR coating for Si surface. A comparison of experimental reflectance data with calculations for a single TiO_2 nanorod layer deposited at $\phi_f = 75°$ on Si substrate is shown in Fig. 3. The strong FP oscillations are characteristic of nanorod layer thickness and n of the medium. The s-polarized component of the reflectance increases with increasing incident angle while the p-polarized component decreases. Only the real part of n is used to simulate reflectance data. The refractive index is found to be the same for all the incident angles, as shown in Fig. 3.

These scattered n values were then fitted (see Fig. 4) using a two term Sellmeier dispersion equation as given below, which has the same form as given for TiO_2 bulk crystal [6]:

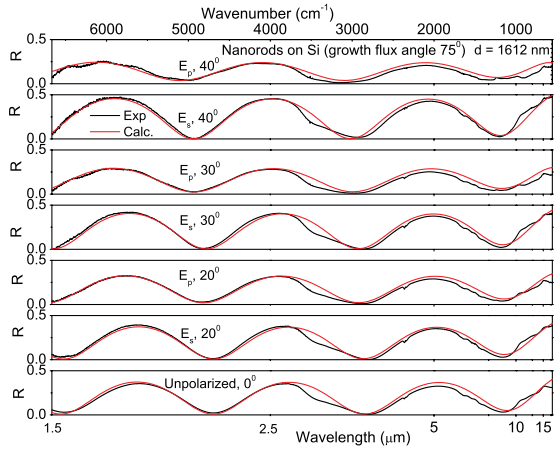

Fig. 3. (Color online) Comparison of experimental reflection spectra with calculations for a TiO_2 nanorod film deposited at $\phi_f = 75°$ on Si substrate. Here, s-polarized component (E_s) increases with increasing incident angle while E_p decreases.

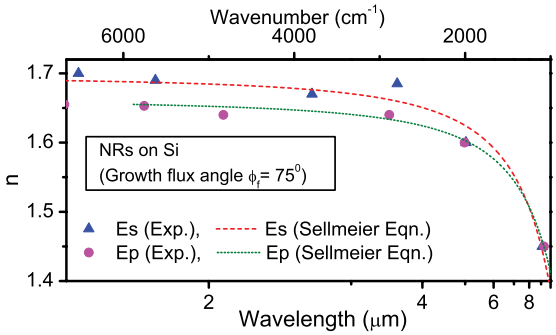

Fig. 4. (Color online) Refractive index obtained for a TiO_2 nanorod layer grown on Si. The dots represent the values found at FP peak positions. The dotted and dashed curves show the corresponding Sellmeier equation obtained by least-square fitting.

$$n^2(\lambda) = A + \frac{B\lambda^2}{\lambda^2 - C^2}. \quad (1)$$

The dots in Fig. 4 represent the values found at FP peak positions. The dotted and dashed curves correspond to the Sellmeier equation obtained by least-square fitting. The Sellmeier coefficients are listed in Table 1.

With this information, the feasibility of a numerical design of multilayer AR coatings on group III–V (such as GaN [7]) based mid-infrared detectors is discussed. In theory, infinite number of layers with a graded refractive index profile will reduce the interface reflection to a near zero and consequently the total reflection. However, fifteen layers per quarter-wave optical thickness (d_{opt}) is generally more than adequate [8]. In fact, FP oscillations play a major role in light transmitted at particular wavelengths. In other words, depending on the thickness and n of the layers, the overall reflection and transmission will get increased or reduced at certain wavelengths. It is possible to fine tune the thickness of each layer and the number of layers to minimize the overall reflection by enhancing destructive interference in the multilayer structure.

A refractive-index profile of a 15-layer stack on GaN substrate is considered for simulation of an AR coating. Here, $n_{GaN} = 2.3$ [9] for the given IR region and $\Delta n = 0.1$ for adjacent layers. All the sublayers have the thickness of 0.4 μm. The abovementioned d_{opt} was chosen by reducing the overall reflection. At longer wavelengths the deterioration increases, because the d_{opt} will approach a half-wave and then the layers will become absentee layers. At shorter wavelengths the overall thickness of the structure will no longer be large enough. Also, the performance depends on Δn. The average reflectance remains less than 1.2% for normal incidence compared

Table 1. Sellmeier Coefficients for *S*- and *P*-Polarized Light [from Eq. (1)] as Determined from Least-Squares Fit to the Experimental Data Points as Shown in Fig. 4[a]

	A	B	C
E_s	2.876(0.002)	77.01(0.05)	90.42(0.05)
E_p	2.754(0.002)	77.27(0.05)	101.49(0.05)

[a]The tolerance is given in the parenthesis.

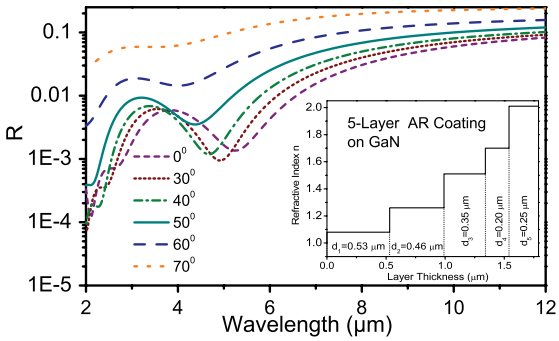

Fig. 5. (Color online) Reflection from five-layer AR coating structures (on GaN substrate) at oblique angles of incidence. For clarity, the curves for incident angles of 10° and 20° are not shown as they are very close to the curves for 0°. The inset shows the graded refractive index (n) profile of the AR coating from air to GaN ($n_{\mathrm{GaN}} = 2.3$) with thickness (d_i) of each layer.

to >16% without the coating. Also, reflectance is less than 5.5% even at 60° across the whole 2–12 μm spectral region. Next, the 15-layer stack is truncated to a five-layer AR coating. In designing this structure, the initial layer parameters were obtained from a similar five-layer stack [1] grown on AlN substrate, which was optimized using a quintic refractive-index profile [8] in the visible spectral region. However, these parameters needed to be modified for the IR region of our interest. Beginning with the first layer, n for each layer is then separately adjusted to minimize the broad reflectivity. After individual layer optimization, the new index is retained for use with subsequent layer optimizations. After the last layer, the process is repeated starting again with the first layer until the overall reflectance converge to a minimum. The same process is then carried out to optimize n for each layer. These two processes are repeated to optimize the layer parameters. The index distribution profile and corresponding average reflectance at oblique angles of incidence are shown Fig. 5. The reflectance remains less than 3.3% for normal incidence for 2–8 μm spectral range and less than 10.5% even at 60° for the same spectral range. For a somewhat narrower spectral region, a better solution for the same overall coating thickness or even thinner solution can be obtained. Also, other methods, such as genetic algorithms [10,11], could be useful to improve AR coating designs.

As long as the substrates can sustain room temperature in a high vacuum environment, and will not chemically react with the depositing material/vapor, nanorods can be deposited onto any flat substrate by OAD. From the deposition point of view, the OAD process is a physical deposition technique and deposition is carried out at room temperature. The growth is dominated by self-shadowing effect, and as demonstrated in literature [12,13], by depositing TiO_2 on various substrates, such as Si, glass, stainless steel (SST), poly-di-methyl-siloxane (PDMS), polyethylene terephthalate (PET), and plastic. Hence, TiO_2 and SiO_2 nanorods could be deposited onto the GaN substrate with thickness precision of ≤1 nm, which can be determined by the deposition method and the deposition control system. Here, an electron beam evaporation system, with the deposition rate controlled to be 0.3 nm /s, and monitored by a quartz crystal microbalance system, is used. From optical property point of view, ϕ_f determines the porosity of the structures, and therefore determines the effective n. It has been reported [1] that n of a TiO_2 nanorod layer can be varied from 2.7 to 1.3 by changing ϕ_f. The n of a SiO_2 nanorod layer can be varied from 1.46 to 1.05. Therefore, a combination of TiO_2 and SiO_2 nanorod layers can be used to grow the designed multilayer AR coating.

In summary, TiO_2 nanorods grown on glass and Si substrates have been optically characterized to extract their complex n profile in the visible and infrared regions. Numerical examples for multilayer AR coatings have been presented for air–GaN interface of an infrared detector ($n = 1$ to 2.3) for 2–12 μm spectral region. Similar results can also be obtained for any other interface (such as, air–GaAs and air–InP). An optimized five-layer AR coating having a graded n profile is presented.

This material is based upon work supported by, or in part by, the U. S. Army Research Laboratory and the U. S. Army Research Office under contract/grant number W911NF-08-1-0448. H. Zhu acknowledges the support from China Scholarship Council. The authors thank Dr. Yanfeng Lao for fruitful discussions.

References

1. J.-Q. Xi, M. F. Schubert, J. K. Kim, E. F. Schubert, S.-Y. Chen, M. Lin, W. Liu, and J. A. Smart, Nat. Photonics **1**, 176 (2007).
2. H. Zhu, W. Cao, G. K. Larsen, R. Toole, and Y. P. Zhao, J. Vac. Sci. Technol. B **30**, 030606 (2012).
3. R. Messier, V. Venugopal, and P. Sunal, J. Vac. Sci. Technol. A **18**, 1538 (2000).
4. M. Born and E. Wolf, *Principles of Optics: Electromagnetic Theory of Propagation, Interference and Diffraction of Light*, 7th ed. (Cambridge Univ., 1999).
5. Y. C. A. Djurisic and E. H. Li, Mater. Sci. Eng., R **38**, 237 (2002).
6. M. Bass, C. DeCusatis, J. Enoch, G. Li, V. N. Mahajan, V. Lakshminarayanan, E. V. Stryland, and C. MacDonald, *Handbook of Optics*, 3rd ed. (McGraw-Hill, 2009).
7. R. C. Jayasinghe, G. Ariyawansa, N. Dietz, A. G. U. Perera, S. G. Matsik, H. B. Yu, I. T. Ferguson, A. Bezinger, S. R. Laframboise, M. Buchanan, and H. C. Liu, Opt. Lett. **33**, 2422 (2008).
8. W. H. Southwell, Opt. Lett. **8**, 584 (1983).
9. New semiconductor materials, available at http://www.ioffe.ru/SVA/NSM/.
10. S. Martin, J. Rivory, and M. Schoenauer, Appl. Opt. **34**, 2247 (1995).
11. M. F. Schubert, F. W. Mont, S. Chhajed, D. J. Poxson, J. K. Kim, and E. F. Schubert, Opt. Express **16**, 5290 (2008).
12. J. P. Singh, H. Chu, J. Abell, R. A. Tripp, and Y. Zhao, Nanoscale **4**, 3410 (2012).
13. D. J. Poxson, F. W. Mont, M. F. Schubert, J. K. Kim, and E. F. Schubert, Appl. Phys. Lett. **93**, 101914 (2008).